

Exotic physical properties in metallic perovskite  $\text{LaRuO}_3$ : Strong evidence for Hund metal

Z. Y. Li,<sup>1</sup> X. Y. Li,<sup>1</sup> J. M. He,<sup>1</sup> Michael A. McGuire,<sup>2</sup> Adam A. Aczel,<sup>3</sup> J. A. Alonso,<sup>4</sup> M. T. Fernandez-Diaz,<sup>5</sup> and J.-S. Zhou,<sup>1,\*</sup>

<sup>1</sup>Materials Science and Engineering Program, Department of Mechanical Engineering,

University of Texas at Austin, Austin, Texas 78712, USA

<sup>2</sup>Materials Science and Technology Division, Oak Ridge National Laboratory, Oak Ridge, Tennessee 37831, USA

<sup>3</sup>Neutron Scattering Division, Oak Ridge National Laboratory, Oak Ridge, Tennessee 37831, USA

<sup>4</sup>Instituto de Ciencia de Materiales de Madrid, CSIC, Cantoblanco, E-28049 Madrid, Spain

<sup>5</sup>Institut-Laue-Langevin (ILL) 156X, F-38042 Grenoble Cedex 9, France



(Received 12 March 2022; accepted 22 July 2022; published 8 August 2022; corrected 7 October 2022)

The Hund's coupling rule is of fundamental importance in atomic physics. It also plays a key role in the determination of physical properties in strongly correlated electron systems where the Fermi energy lies in multiple bands. We report a thorough investigation of a rarely studied 4d perovskite oxide  $\text{LaRuO}_3$  by a suite of measurements including transport, magnetization, specific heat, thermoelectric power, thermal conductivity, and neutron and x-ray diffraction. Our results are consistent with theoretical predictions, which makes  $\text{LaRuO}_3$  an exemplary Hund metal.

DOI: [10.1103/PhysRevB.106.L081104](https://doi.org/10.1103/PhysRevB.106.L081104)

The Hartree-Fock (HF) approximation lays the foundation for treating many-body systems with single-body theory. The approach incorporates Coulomb interactions and spin-spin correlations between electrons at the mean field level and each electron is assigned the same spin that is delocalized in a short radius sphere in real space. In strongly correlated systems, the Coulomb interaction increases the probability for electrons to stay in the atomic orbitals in the Bloch waves. The real space confinement for electrons leads to a gap between the occupied and empty bands, i.e., the Mott transition. In a system where the Fermi energy crosses the bands arising from multiple orbitals, the Hund's coupling rule from atomic physics must be brought into the picture, which leads to a Hund metal. In this case, Hund's coupling regulates the magnitude of the spins, competes with the interatomic spin-spin interaction, and reduces the quasiparticle lifetime. A characteristic and measurable property for a Hund metal is the thermally driven transition from coherent to incoherent state in which spins become localized [1–3]. The Hund metal has drawn attention since 2008. The model has been applied to rationalize physical properties observed in iron pnictide superconductors  $\text{KFe}_2\text{As}_2$  [4] and  $\text{Sr}_2\text{RuO}_4$  [5–9]. Whereas the transition of the transport property from the Fermi-liquid to a non-Fermi-liquid behavior in  $\text{KFe}_2\text{As}_2$  and the thermally driven disappearing of the quasiparticle state from angle-resolved photoemission spectroscopy (ARPES) in  $\text{Sr}_2\text{RuO}_4$  have been reported [6,7], the key feature of localized spin has been generally missing in these materials [10–12]. In this Letter, we report a comprehensive set of measurements on the rarely studied metallic perovskite  $\text{LaRuO}_3$ . An extremely strong intra-atomic inter-

action in the oxide enhances the Hund's coupling and ensures that  $\text{LaRuO}_3$  represents an extreme case of a Hund metal.

In comparison with the well-known ferromagnetic metal  $\text{SrRu}^{4+}\text{O}_3$  [13–25], the perovskite  $\text{LaRuO}_3$  has been rarely studied since  $\text{Ru}^{3+}$  is metastable in oxides.  $\text{LaRuO}_3$  is the only member of the perovskite family  $RR\text{RuO}_3$  that can be synthesized at ambient pressure [26–28]. High-pressure synthesis is needed for obtaining the entire family of polycrystalline  $RR\text{RuO}_3$  samples [29–31]. By using the spark plasma sintering, we demonstrated that the high density  $RR\text{RuO}_3$  pellet samples can be synthesized for  $R = \text{La}$  and  $\text{Pr}$ . The resistivity of the  $\text{LaRuO}_3$  sample is quite low compared to results reported in the literature. Detailed information about the sample synthesis and the characterization is provided in the Supplemental Material (SM) [32]. These oxides crystallize in the orthorhombic perovskite structure with the space group  $Pnma$ . The structural distortion originates from the cooperative octahedral-site rotations which bend the Ru-O-Ru bond angle  $\psi$  from  $180^\circ$ . As a direct measurement of the orthorhombic distortion, the separation between lattice parameters  $a$  and  $c$  increases with increasing of the  $\text{Pr}$  doping  $x$  in  $\text{La}_{1-x}\text{Pr}_x\text{RuO}_3$ ; see Fig. S2 in the SM [32]. By tuning the rare earth substitution, a reduction of electronic bandwidth in  $\text{La}_{1-x}\text{Pr}_x\text{RuO}_3$ , which is proportional to  $\cos \psi$ , leads to an evolution from metallic  $\text{LaRuO}_3$  to an insulating  $\text{PrRuO}_3$  [29]. The cell volume decreases gradually with increasing  $x$ , which resembles closely the cell volume change in the diamagnetic insulators  $\text{La}_{1-x}\text{Pr}_x\text{GaO}_3$ ; see Fig. S2 in the SM [32]. This observation is in sharp contrast to the first-order Mott transition found in  $R\text{NiO}_3$  [33,34]. Moreover, no magnetic transition has been detected to the lowest temperature from metallic  $\text{LaRuO}_3$  to insulator  $\text{PrRuO}_3$ , see the results of neutron diffraction and specific heat in the SM [32].

\*Corresponding author: jszhou@mail.utexas.edu

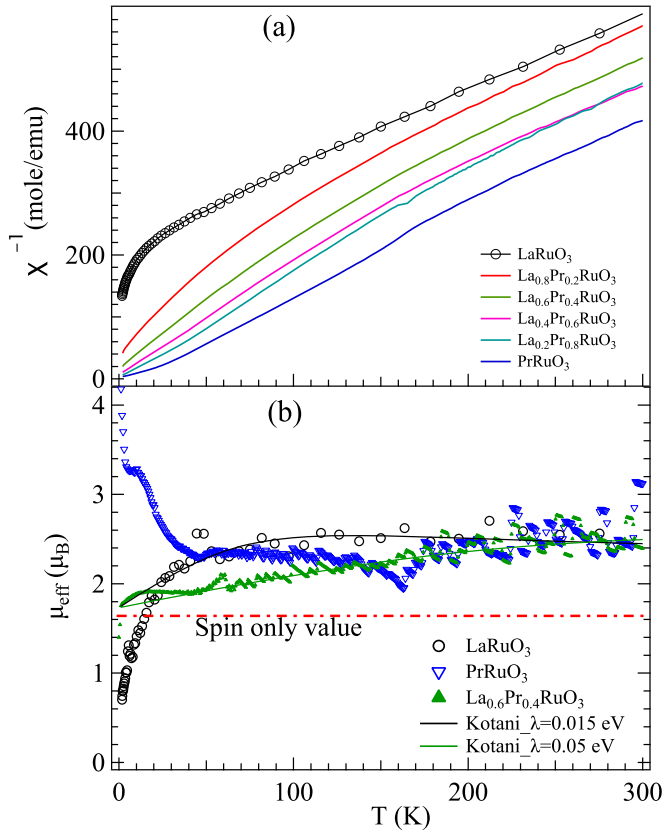


FIG. 1. (a) Temperature dependence of (a) inverse magnetic susceptibility of  $\text{La}_{1-x}\text{Pr}_x\text{RuO}_3$  and (b)  $\mu_{\text{eff}} = \sqrt{8C}$  derived from (a) in the plot of  $\chi = C/T$ . Solid lines in (b) from the Kotani's theory with different values of spin-orbit coupling. The dash-point line in the plot is the spin-only value of  $\mu_{\text{eff}}$  in a Curie law for a system with  $n = 1$  or 5.

Understanding the magnetic susceptibility  $\chi$  is the first step for elucidating the physics in  $\text{LaRuO}_3$ . Figure 1(a) shows the temperature dependence of  $\chi^{-1}$  for the series of  $\text{La}_{1-x}\text{Pr}_x\text{RuO}_3$ . Fitting  $\chi^{-1}(T)$  to a Curie-Weiss law seems to work reasonably well for  $T > 100$  K. However, a large Weiss constant  $\theta = -182.1$  K, a larger  $\mu_{\text{eff}} = 2.556 \mu_B$  than the spin-only value, and a nonlinear  $\chi^{-1}(T)$  below 100 K make the practice questionable. Given that the spin-orbit coupling (SOC) is strong for the  $4d$  electrons and the orbital angular momentum is not quenched in the low spin  $\text{Ru}^{3+} \cdot t_{2g}^5$ , the influence of SOC must be considered. The Curie-Weiss law is the extreme case in the general formula of magnetic susceptibility for a negligible SOC [35,36]. By working on a Hamiltonian for isolated magnetic ions, which includes single-electron, spin-orbit coupling, and Zeeman effect contributions, Kotani [37] was able to derive an analytical expression for the magnetic susceptibility of compounds containing isolated  $4d$  or  $5d$  magnetic ions. In the Curie law expression  $\chi(T) = C/T$ , the  $\mu_{\text{eff}} \approx \sqrt{8C}$  becomes temperature dependent. Kotani's modified expression for the effective magnetic moment in the system with  $n = 5$  is

$$\mu_{\text{eff}}^2 = \frac{3x + 8 - 8e^{-\frac{3}{2}x}}{x(1 + e^{-\frac{3}{2}x})}, \quad (1)$$

where  $x = \lambda/kT$  and  $\lambda$  is the spin-orbit coupling.

The  $\mu_{\text{eff}}(T)$  of  $\text{LaRuO}_3$  shown in Fig. 1(b) becomes temperature dependent below 100 K. Over a broad range of temperature, the  $\mu_{\text{eff}} = 2.556 \mu_B$  of  $\text{LaRuO}_3$  is clearly larger than the spin-only value for a  $d^5$  low spin system. However,  $\mu_{\text{eff}}(T)$  of  $\text{LaRuO}_3$  matches the expression in Eq. (1) for a  $d^5$  system by the Kotani theory stunningly well. Kotani's theory has been applied to successfully describe the magnetic susceptibility in insulators with isolated  $4d$  or  $5d$  magnetic ions [38,39]. It is surprising that the theory works well in the metallic  $\text{LaRuO}_3$ . The best fitting of the experimental  $\mu_{\text{eff}}$  at  $T > 30$  K to Kotani's theory is obtained with  $\lambda = 0.015$  eV, which is much smaller than  $\lambda = 0.07$  eV for insulators with isolated  $\text{Ru}^{3+}$  [39]. The larger radial extension of the wave function reduces the atomic SOC parameter  $\lambda$  by a multiplicative fraction  $k_c < 1$  (i.e.,  $k_c \lambda L \cdot S$ ) [40]. The  $\mu_{\text{eff}}$  predicted by the Kotani theory decreases with decreasing temperature and reaches  $1.73 \mu_B$  at 0 K. The  $\mu_{\text{eff}}$  of  $\text{LaRuO}_3$  deviates from the theoretical curve below  $\sim 30$  K. Since spins in  $\text{LaRuO}_3$  do not order at low temperatures down to 1.5 K (see Fig. S4 in the SM [32]), the deviation of  $\mu_{\text{eff}}(T)$  from Kotani's theory at  $T < 30$  K may indicate a change of the electronic structure. This observation will be further discussed in connection with anomalies found in other physical properties.

The Pr substitution in  $\text{La}_{1-x}\text{Pr}_x\text{RuO}_3$  increases the structural distortion; specifically, the Ru-O-Ru bond angle decreases further from  $180^\circ$  [30]. The same chemical substitution in  $\text{La}_{1-x}\text{Pr}_x\text{NiO}_3$  leads to a metal-insulator transition at the Néel temperature in  $\text{PrNiO}_3$  [33]. As  $x$  increases in  $\text{La}_{1-x}\text{Pr}_x\text{RuO}_3$ , the inverse  $\chi(T)$  lowers progressively whereas the slope does not show an obvious change in Fig. 1(a). The  $\mu_{\text{eff}}(T)$  of  $\text{La}_{1-x}\text{Pr}_x\text{RuO}_3$  changes very little with  $x$  near room temperature as shown in Fig. 1(b). The  $\mu_{\text{eff}}(T)$  of  $\text{La}_{0.6}\text{Pr}_{0.4}\text{RuO}_3$  can be fit to Kotani's theory with  $\lambda = 0.05$  eV over the entire range of temperature. An increased  $\lambda$  in the Pr-doped sample relative to that for  $\text{LaRuO}_3$  is consistent with the bandwidth reduction reflected in the higher resistivity in the Pr-doped samples in Fig. 2. For  $\text{PrRuO}_3$ , there is a small amount of the impurity phase  $\text{Pr}_2\text{Ru}_2\text{O}_7$  (see Fig. S1 in the SM [32]) which contributes to the anomaly at 160 K and an upturn below 50 K in the  $\chi^{-1}(T)$  of Fig. 1(b). The question here is why the magnetic susceptibility of metallic  $\text{LaRuO}_3$  fits the model of single-ion physics. The physical picture of the anomalous metal could be uncovered through the analysis of transport properties and perhaps more intuitively from the thermal conductivity.

Figure 2(a) shows the resistivity  $\rho(T)$  of  $\text{La}_{1-x}\text{Pr}_x\text{RuO}_3$ . The Pr doping in  $\text{La}_{1-x}\text{Pr}_x\text{RuO}_3$  leads to an evolution from a metal in  $\text{LaRuO}_3$  to an insulator in  $\text{PrRuO}_3$ . In addition to having an activated behavior, the  $\rho(T)$  of  $\text{PrRuO}_3$  increases by nearly two orders of magnitude at 2 K. Plotted on a linear scale in Fig. 1(b), the  $\rho(T)$  of  $\text{LaRuO}_3$  does not behave like a normal metal. There is a clear inflection point of  $\rho(T)$  near  $T^* = 30$  K. Fitting the  $\rho(T)$  of  $\text{LaRuO}_3$  below 10 K to a power law  $\rho(T) = \rho_0 + AT^n$  gives  $n = 1.9$ , which implies a Fermi liquid state (this trend persists even down to 50 mK; see Fig. S8 in the SM [32]). The curvature change of  $\rho(T)$  at 30 K may resemble the coherent to incoherent state transition predicted for a Hund metal and observed in the iron pnictide superconductors [1–4]. The transition temperature  $T^*$  also coincides with the tempera-

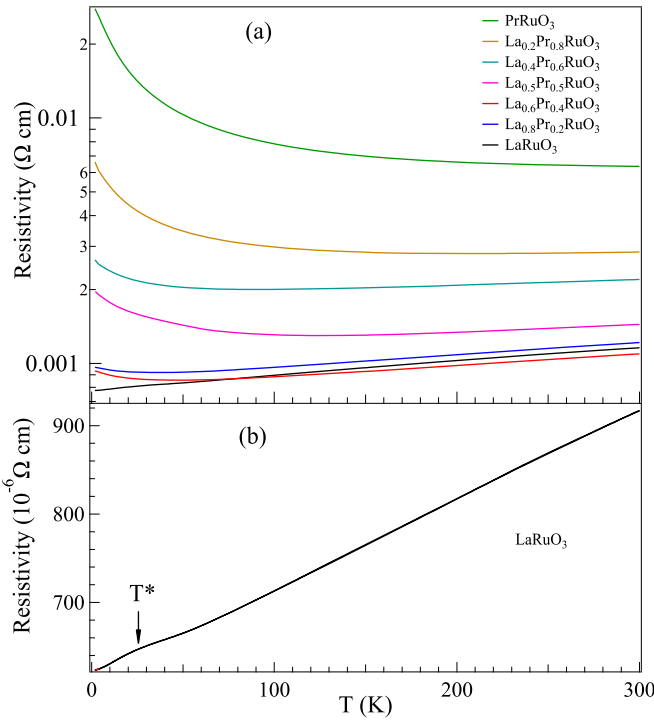


FIG. 2. Temperature dependence of the resistivity in  $\text{La}_{1-x}\text{Pr}_x\text{RuO}_3$ . A slightly higher resistivity of  $\text{LaRuO}_3$  than that of  $\text{La}_{0.8}\text{Pr}_{0.2}\text{RuO}_3$  at room temperature may be caused by the geometry uncertainty of the samples and the distance between the voltage leads in the four-probe measurement. The resistivity drop of  $\text{LaRuO}_3$  on cooling through  $T^*$  in the linear scale plot shown in (b) resembles the feature expected for the incoherent to coherent state transition as predicted by the theory.

ture where  $\mu_{\text{eff}}(T)$  deviates from Kotani's theory on cooling through  $T^*$ .

Figure 3(a) shows the thermoelectric power  $S(T)$  of  $\text{LaRuO}_3$ . The overall temperature dependence fits the description for a metal, i.e.,  $S \approx C_{\text{el}}/e = (\gamma/e)T$  at  $T \ll \theta_D$  (Debye temperature) and the slope being reduced to  $\sim(\gamma/3e)$  at high temperatures [41]. Based on the diffusive formula  $S = (\frac{\pi^2 k^2}{e E_F})T$  and  $E_F \approx 2 \text{ eV}$  from the band structure calculation in Fig. 4, and Fig. S9 in the SM [32], a  $S \approx 0.037T \text{ } (\mu\text{V/K})$  is obtained. A much-enhanced slope in the  $S(T) = 0.36T \text{ } (\mu\text{V/K})$  at low temperatures indicates a strong renormalization which gives rise to a flat band at  $E_F$  due to strong correlations, which is supported by a much-enhanced  $\gamma$  of electronic contribution to the specific heat relative to that from the density functional theory (DFT) calculation (discussed below).  $S(T)$  is perfectly linear at low temperatures; a deviation from the linear behavior occurs above 30 K which coincides with  $T^*$  where the  $\rho(T)$  goes through an inflection point. A transition from a linear  $S(T)$  to a nonlinear  $S(T)$  appears to be relevant to the coherent state to incoherent state transition. A  $\sim 40 \text{ } (\mu\text{V/K})$  for  $\text{LaRuO}_3$  is the largest thermoelectric power at room temperature among the single-valent metallic perovskites [42,43] which could be justified by the Fermi energy at the top of the  $t_{2g}$  orbital band; see the band calculation result with DFT+ $U$  in Fig. S9 in the SM [32]. Whereas there is a crossover from

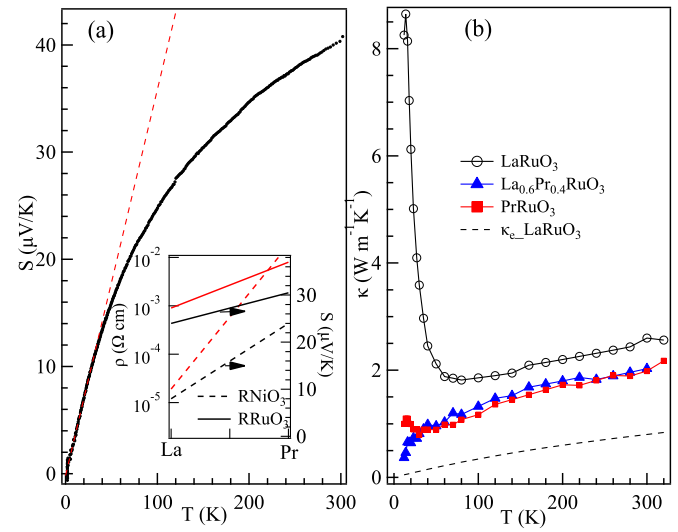


FIG. 3. Temperature dependence of (a) the thermoelectric power for  $\text{La}_{1-x}\text{Pr}_x\text{RuO}_3$ ; the inset shows the changes of resistivity and thermoelectric power at 100 K from  $R = \text{La}$  to  $\text{Pr}$  in  $RR\text{O}_3$  and  $R\text{NiO}_3$  and (b) the thermal conductivity of  $\text{La}_{1-x}\text{Pr}_x\text{RuO}_3$ .

a metallic phase in  $\text{LaRuO}_3$  to an insulating phase in  $\text{PrRuO}_3$ , as shown by a huge increase of the resistivity in Fig. 2, Pr substitution in  $\text{La}_{1-x}\text{Pr}_x\text{RuO}_3$  only leads to a modest increase of the thermoelectric power and no obvious change in the temperature dependence as shown in the inset of Fig. S5 [32], which is in sharp contrast to a huge increase on crossing the metal-insulator transition in the single-band system  $R\text{NiO}_3$  [44,45]. The changes in the resistivity and the thermoelectric power at 100 K on crossing the metal-insulator transition as  $R = \text{La}$  is replaced by  $\text{Pr}$  in perovskite systems  $R\text{NiO}_3$  and  $RR\text{O}_3$  are shown as an inset of Fig. 3(a). The thermoelectric power in an insulator is sensitive to the charge carrier density. A drastic change of  $S$  on crossing the metal-insulator transition from  $\text{LaNiO}_3$  to  $\text{PrNiO}_3$  at 100 K corresponds to a gap opening at the Fermi energy. In contrast, a gradual change of  $S$  from metallic  $\text{LaRuO}_3$  to an insulating phase of  $\text{La}_{1-x}\text{Pr}_x\text{RuO}_3$  implies that the crossover from a metal to an insulator is driven by disorder. As the bandwidth narrows with increasing Pr doping in  $\text{La}_{1-x}\text{Pr}_x\text{RuO}_3$ , the transportation of charge carriers changes from scattering in the metallic phase with incoherent electrons to diffusion or hopping in the insulator phase with localized electrons.

The thermal conductivity measurement provides further useful information for characterizing the incoherent state and the coherent to incoherent state transition. Figure 3(b) shows the lattice thermal conductivity  $\kappa$  after correcting for the electronic contribution via the Wiedemann-Franz law. The  $\kappa(T)$  of  $\text{LaRuO}_3$  at room temperature is much lower than that of typical single-valent insulator perovskites such as  $\text{LaGaO}_3$  [46] and metallic perovskites such as  $\text{LaNiO}_3$  and  $\text{LaCuO}_3$  [43]. For  $T > 100 \text{ K}$ , the  $\kappa(T)$  of  $\text{LaRuO}_3$  exhibits glassy behavior. In a crystalline material, Cahill *et al.* [47] have shown that disorder can significantly suppress the  $\kappa(T)$ ; the low limit of  $\kappa(T)$  in a disordered crystal can reach the level for amorphous materials. Disorder in the perovskite  $\text{LaRuO}_3$  can be induced by impurities in the lattice or arise because of

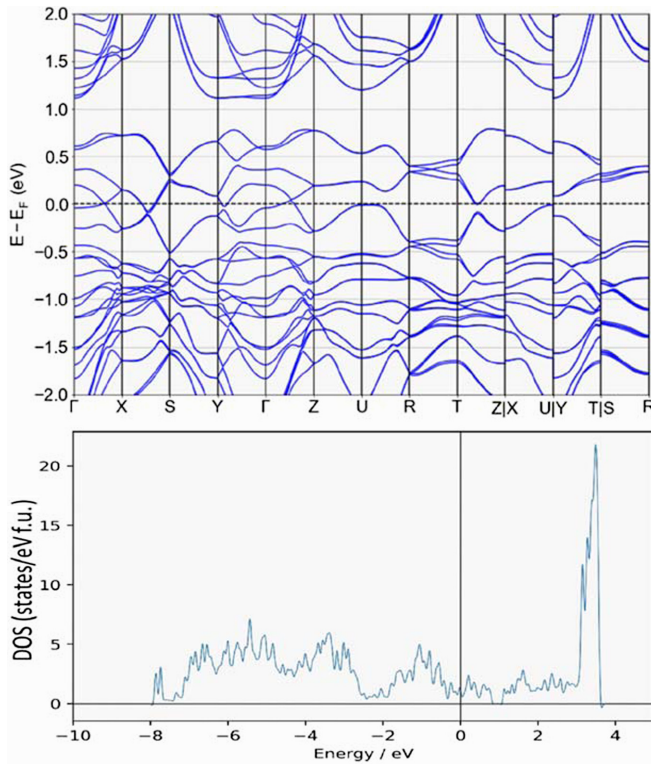


FIG. 4. The band structure (upper panel) and the density of states of  $\text{LaRuO}_3$  (lower panel) from the DFT calculation. The band structure shown here has been obtained by adding  $U$  and spin-orbit coupling (SOC) in the calculation. The calculation without SOC gives rise to an insulator of  $\text{LaRuO}_3$ ; see Fig. S9 in the SM [32] for the result and detailed information about the calculation.

strong electron-phonon interactions, which leads to polaron physics. A sharp upturn of  $\kappa(T)$  below 60 K rules out the first possibility. The upturn of  $\kappa(T)$  near  $T^*$  implies that the phonon thermal conductivity is restored in the coherent state of electrons where the electron-phonon becomes relatively weak. In contrast, electrons in the incoherent state behave like large polarons which interact strongly with the lattice so as to significantly reduce the phonon mean free path to the level of interatomic distance. As a result,  $\kappa(T)$  is suppressed in the incoherent phase. The high temperature limit  $T^*$  for the coherent electrons is determined by the bandwidth.  $T^*$  drops upon the Pr substituting, which explains why there is no upturn of  $\kappa(T)$  in all Pr-doped samples and the end member  $\text{PrRuO}_3$ . The hopping conduction leads to a further decrease of  $\kappa(T)$  in all the samples of  $\text{La}_{1-x}\text{Pr}_x\text{RuO}_3$  with  $x > 0$ .

The band structure of  $\text{LaRuO}_3$  from DFT calculation in Fig. 4, and Fig. S9 in the SM [32], indicates the multiband crossing at the Fermi energy, which makes  $\text{LaRuO}_3$  legitimate as a Hund metal. The specific heat measurement shown in Fig. S7 [32] can be fit to the formula  $C_p = \gamma T + \beta T^3$  at low temperatures with  $\gamma = 41 \text{ mJ}/(\text{K}^2 \text{ mole})$ . A large ratio of  $\gamma/\gamma_0 \approx 16$ , with  $\gamma_0 = 2.6 \text{ mJ}/(\text{K}^2 \text{ mole})$ , obtained from the band structure in Fig. 4, provides strong evidence for the importance of Hund's coupling in  $\text{LaRuO}_3$  as predicted theoretically by Haule and Kotliar [1].

The Bloch function for describing electrons in a solid consists of plane wave and atomic wave function contributions. The concept of quasiparticles addresses the many-body correlations, but the quasiparticle lifetime is subject to the on-site correlation energy  $U$ . In the presence of strong Hund's coupling, the quasiparticle lifetime is severely modulated in a multiple-orbital system depending on the band filling number  $n$ . In a cubic perovskite oxide model system with a partially filled, low spin  $\pi^*$  band, de' Medici *et al.* [3] have provided the numerical solution of the Kanamori Hamiltonian. For  $n = 1, 2, 3, 4$  the effect of Hund's coupling is to increase the threshold  $U_c$  for the Mott transition, whereas  $U_c$  is much reduced for  $n = 3$ . A characteristic temperature  $T^*$  in the phase diagram marks the temperature above which the quasiparticle lifetime becomes sufficiently short and the coherent state is lost. In the incoherent state, while metallicity remains, the probability of finding charge carriers within the atomic wave functions is significantly high. As a result, the screening on magnetic moments becomes weak and a Curie-Weiss law is expected in the paramagnetic susceptibility [1]. The spin freezing for the incoherent electrons has been derived in a calculation by Werner *et al.* [2]. Specifically, Haule and Kotliar [1] have shown the influence of Hund's rule coupling in  $\chi(T)$  and  $\rho(T)$  for iron oxypnictides. For  $J_H > 0.4 \text{ eV}$ , the transition from the incoherent state to the coherent state is represented by the drop in resistivity. A Curie law behavior is predicted for the magnetic susceptibility in the incoherent phase with  $J_H > 0.4 \text{ eV}$ . These authors have also shown that the electronic contribution to the specific heat  $\gamma$  is greatly enhanced as  $J_H$  increases.

$\text{LaRuO}_3$  has the low spin  $d^5$  electron configuration in a nearly cubic crystal field. Its physical properties are all consistent with the theoretical predictions for a Hund metal. Whereas a Curie-Weiss law behavior or highly localized moment in the incoherent state has been predicted for a Hund metal, there have been few reports of experimental verifications.  $\text{LaRuO}_3$  is the only metal showing the paramagnetic susceptibility fitting a model of single-ion physics. In addition, disordered electrons in the incoherent state destroy the phonon quasiparticles via strong electron-phonon interactions in this narrow-band system, which suppresses the phonon thermal conductivity. As shown in the theoretical calculation [3],  $U_c$  for a  $d^5$  system is large. An increase of  $U$  by the Pr substituted  $\text{La}_{1-x}\text{Pr}_x\text{RuO}_3$  is insufficient to trigger a Mott transition in this case. Instead, the gradual crossover from a metallic  $\rho(T)$  in  $\text{LaRuO}_3$  to an activated  $\rho(T)$  in  $\text{PrRuO}_3$  is more likely due to Anderson localization by disorder. This argument is supported by a gradual change of the thermoelectric power in the crossover from metallic  $\text{LaRuO}_3$  to an insulator  $\text{PrRuO}_3$ , which is in sharp contrast to what is found in the single-band system of  $\text{RNiO}_3$  which exhibits a Mott transition as the bandwidth is reduced.

In conclusion, the strong intra-atomic interaction restores the Hund's coupling  $J_H$  in metallic  $\text{LaRuO}_3$ . A strong  $J_H$  reduces the quasiparticle lifetime, which is manifested by a transition from a coherent to an incoherent electronic phase from the measurement of resistivity. Moreover, the effect of  $J_H$  is to create localized spins in the incoherent phase. In  $\text{LaRuO}_3$ , the paramagnetic susceptibility in the incoherent

phase can be described by a model of single-ion physics. Since the threshold  $U_c$  for the Mott transition is significantly enlarged for the low spin system with  $n = 5$  due to  $J_H$ , the bandwidth reduction in  $\text{La}_{1-x}\text{Pr}_x\text{RuO}_3$  series does not lead to a Mott transition, but an evolution from the metallic phase of incoherent electrons to an insulating phase by disorder. Electrons in the incoherent phase of  $\text{LaRuO}_3$  disturb the phonon structure due to a strong electron-phonon coupling, which leads to a glassy thermal conductivity. The phonon thermal conductivity is restored in the coherent phase below  $T^*$ . All these observations make  $\text{LaRuO}_3$  a representative Hund metal.

This research was primarily supported by NSF MRSEC Grants No. DMR-1720595 and No. DMR-1949701. J.-S.Z. is grateful to John Goodenough for the encouragement and the long-term support. J.A.A. thanks the Spanish Ministry for Science and Innovation (MCIN/AEI/10.13039/501100011033) for granting the Project No. PID2021-122477OB-I00. M.A.M. acknowledges support from the US Department of Energy, Office of Science, Basic Energy Sciences, Materials Sciences and Engineering Division. A portion of this research used resources at the High Flux Isotope Reactor, which is a DOE Office of Science User Facility operated by Oak Ridge National Laboratory.

---

[1] K. Haule and G. Kotliar, Coherence–incoherence crossover in the normal state of iron pnictides and importance of Hund’s rule coupling, *New J. Phys.* **11**, 025021 (2009).

[2] P. Werner, E. Gull, M. Troyer, and A. J. Millis, Spin Freezing Transition and Non-Fermi-Liquid Self-Energy in a Three-Orbital Model, *Phys. Rev. Lett.* **101**, 166405 (2008).

[3] L. de’ Medici, J. Mravlje, and A. Georges, Janus-Faced Influence of Hund’s Rule Coupling in Strongly Correlated Materials, *Phys. Rev. Lett.* **107**, 256401 (2011).

[4] F. Hardy, A. E. Böhmer, D. Aoki, P. Burger, T. Wolf, P. Schweiss, R. Heid, P. Adelmann, Y. X. Yao, G. Kotliar, J. Schmalian, and C. Meingast, Evidence of Strong Correlations and Coherence-Incoherence Crossover in the Iron Pnictide Superconductor  $\text{KFe}_2\text{As}_2$ , *Phys. Rev. Lett.* **111**, 027002 (2013).

[5] Z. P. Yin, K. Haule, and G. Kotliar, Kinetic frustration and the nature of the magnetic and paramagnetic states in iron pnictides and iron chalcogenides, *Nat. Mater.* **10**, 932 (2011).

[6] T. Kondo, M. Ochi, M. Nakayama, H. Taniguchi, S. Akebi, K. Kuroda, M. Arita, S. Sakai, H. Namatame, M. Taniguchi, Y. Maeno, R. Arita, and S. Shin, Orbital-Dependent Band Narrowing Revealed in an Extremely Correlated Hund’s Metal Emerging on the Topmost Layer of  $\text{Sr}_2\text{RuO}_4$ , *Phys. Rev. Lett.* **117**, 247001 (2016).

[7] J. Mravlje, M. Aichhorn, T. Miyake, K. Haule, G. Kotliar, and A. Georges, Coherence-Incoherence Crossover and the Mass-Renormalization Puzzles in  $\text{Sr}_2\text{RuO}_4$ , *Phys. Rev. Lett.* **106**, 096401 (2011).

[8] J. Mravlje and A. Georges, Thermopower and Entropy: Lessons from  $\text{Sr}_2\text{RuO}_4$ , *Phys. Rev. Lett.* **117**, 036401 (2016).

[9] D. Stricker, J. Mravlje, C. Berthod, R. Fittipaldi, A. Vecchione, A. Georges, and D. van der Marel, Optical Response of  $\text{Sr}_2\text{RuO}_4$  Reveals Universal Fermi-Liquid Scaling and Quasiparticles beyond Landau Theory, *Phys. Rev. Lett.* **113**, 087404 (2014).

[10] A. P. Mackenzie and Y. Maeno, The superconductivity of  $\text{Sr}_2\text{RuO}_4$  and the physics of spin-triplet pairing, *Rev. Mod. Phys.* **75**, 657 (2003).

[11] A. P. Mackenzie, S.-i. Ikeda, Y. Maeno, T. Fujita, S. R. Julian, and G. G. Lonzarich, The Fermi surface topography of  $\text{Sr}_2\text{RuO}_4$ , *J. Phys. Soc. Jpn.* **67**, 385 (1998).

[12] Y. Kamihara, T. Watanabe, M. Hirano, and H. Hosono, Iron-based layered superconductor  $\text{La}[\text{O}_{1-x}\text{F}_x]\text{FeAs}$  ( $x = 0.05–0.12$ ) with  $T_c = 26$  K, *J. Am. Chem. Soc.* **130**, 3296 (2008).

[13] J. M. Longo, P. M. Raccah, and J. B. Goodenough, Magnetic properties of  $\text{SrRuO}_3$  and  $\text{CaRuO}_3$ , *J. Appl. Phys.* **39**, 1327 (1968).

[14] R. J. Bouchard and J. L. Gillson, Electrical properties of  $\text{CaRuO}_3$  and  $\text{SrRuO}_3$  single crystals, *Mater. Res. Bull.* **7**, 873 (1972).

[15] P. Khalifah, I. Ohkubo, H. M. Christen, and D. G. Mandrus, Evolution of transport and magnetic properties near the ferromagnetic quantum critical point in the series  $\text{Ca}_{1-x}\text{Sr}_x\text{RuO}_3$ , *Phys. Rev. B* **70**, 134426 (2004).

[16] K. Fujioka, J. Okamoto, T. Mizokawa, A. Fujimori, I. Hase, M. Abbate, H. J. Lin, C. T. Chen, Y. Takeda, and M. Takano, Electronic structure of  $\text{SrRuO}_3$ , *Phys. Rev. B* **56**, 6380 (1997).

[17] J. Okamoto, T. Mizokawa, A. Fujimori, I. Hase, M. Nohara, H. Takagi, Y. Takeda, and M. Takano, Correlation effects in the electronic structure of  $\text{SrRuO}_3$ , *Phys. Rev. B* **60**, 2281 (1999).

[18] L. Klein, J. S. Dodge, C. H. Ahn, G. J. Snyder, T. H. Geballe, M. R. Beasley, and A. Kapitulnik, Anomalous spin Scattering Effects in the Badly Metallic Itinerant Ferromagnet  $\text{SrRuO}_3$ , *Phys. Rev. Lett.* **77**, 2774 (1996).

[19] A. P. Mackenzie, J. W. Reiner, A. W. Tyler, L. M. Galvin, S. R. Julian, M. R. Beasley, T. H. Geballe, and A. Kapitulnik, Observation of quantum oscillations in the electrical resistivity of  $\text{SrRuO}_3$ , *Phys. Rev. B* **58**, R13318 (1998).

[20] P. Kostic, Y. Okada, N. C. Collins, Z. Schlesinger, J. W. Reiner, L. Klein, A. Kapitulnik, T. H. Geballe, and M. R. Beasley, Non-Fermi-Liquid Behavior of  $\text{SrRuO}_3$ : Evidence from Infrared Conductivity, *Phys. Rev. Lett.* **81**, 2498 (1998).

[21] M. Shepard, S. McCall, G. Cao, and J. E. Crow, Thermodynamic properties of perovskite  $A\text{RuO}_3$  ( $A = \text{Ca}, \text{Sr}, \text{and Ba}$ ) single crystals, *J. Appl. Phys.* **81**, 4978 (1997).

[22] G. Cao, S. McCall, M. Shepard, J. E. Crow, and R. P. Guertin, Thermal, magnetic, and transport properties of single-crystal  $\text{Sr}_{1-x}\text{Ca}_x\text{RuO}_3$  ( $0 \leq x \leq 1$ ), *Phys. Rev. B* **56**, 321 (1997).

[23] Y. Kats, L. Klein, J. W. Reiner, T. H. Geballe, M. R. Beasley, and A. Kapitulnik, Magnetic resistivity in  $\text{SrRuO}_3$  and the ferromagnetic phase transition, *Phys. Rev. B* **63**, 054435 (2001).

[24] F. Fukunaga and N. Tsuda, On the magnetism and electronic conduction of itinerant magnetic system  $\text{Ca}_{1-x}\text{Sr}_x\text{RuO}_3$ , *J. Phys. Soc. Jpn.* **63**, 3798 (1994).

[25] T. He, Q. Huang, and R. J. Cava, Comparison of the magnetic properties of isoelectronic  $\text{Sr}_x(\text{Na}_{0.5}\text{La}_{0.5})_{1-x}\text{RuO}_3$  and  $\text{Sr}_x\text{Ca}_{1-x}\text{RuO}_3$  perovskites, *Phys. Rev. B* **63**, 024402 (2000).

[26] R. J. Bouchard and J. F. Weiher,  $\text{La}_x\text{Sr}_{1-x}\text{RuO}_3$ : A new perovskite series, *J. Solid State Chem.* **4**, 80 (1972).

[27] T. Sugiyama and N. Tsuda, Electrical and magnetic properties of  $\text{Ca}_{1-x}\text{La}_x\text{RuO}_3$ , *J. Phys. Soc. Jpn.* **68**, 3980 (1999).

[28] R. J. Bouchard, J. F. Weiher, and J. L. Gillson, The preparation and properties of  $\text{LaRu}_x\text{Ga}_{1-x}\text{O}_3$  perovskites, *J. Solid State Chem.* **6**, 519 (1973).

[29] H. Kobayashi, M. Nagata, R. Kanno, and Y. Kawamoto, Structural characterization of the orthorhombic perovskites:  $[\text{ARuO}_3$  ( $\text{A} = \text{Ca, Sr, La, Pr}$ )], *Mater. Res. Bull.* **29**, 1271 (1994).

[30] A. Sinclair, J. A. Rodgers, C. V. Topping, M. Míšek, R. D. Stewart, W. Kockelmann, J.-W. G. Bos, and J. P. Attfield, Synthesis and properties of lanthanide ruthenium(III) oxide perovskites, *Angew. Chem., Int. Ed.* **53**, 8343 (2014).

[31] K. Ji, A. Paul, E. Solana-Madruga, A. M. Arevalo-Lopez, U. V. Waghmare, and J. P. Attfield,  $\text{YRuO}_3$ : A quantum weak ferromagnet, *Phys. Rev. Materials* **4**, 091402 (2020).

[32] See Supplemental Material at <http://link.aps.org/supplemental/10.1103/PhysRevB.106.L081104> for details of the structural study by neutron and x-ray diffraction, the sample synthesis, specific heat, magnetoresistance measurement, and electronic structure by first-principles calculation.

[33] J. B. Torrance, P. Lacorre, A. I. Nazzal, E. J. Ansaldo, and Ch. Niedermayer, Systematic study of insulator-metal transitions in perovskites  $\text{RNiO}_3$  ( $\text{R} = \text{Pr, Nd, Sm, Eu}$ ) due to closing of charge-transfer gap, *Phys. Rev. B* **45**, 8209 (1992).

[34] J. Rodríguez-Carvajal, S. Rosenkranz, M. Medarde, P. Lacorre, M. T. Fernández-Díaz, F. Fauth, and V. Trounov, Neutron-diffraction study of the magnetic and orbital ordering in  $\text{SmNiO}_3$  and  $\text{EuNiO}_3$ , *Phys. Rev. B* **57**, 456 (1998).

[35] J. Kanamori, Theory of the magnetic properties of ferrous and cobaltous oxides, I, *Prog. Theor. Phys.* **17**, 177 (1957).

[36] J. Kanamori, Theory of the magnetic properties of ferrous and cobaltous oxides, II, *Prog. Theor. Phys.* **17**, 197 (1957).

[37] M. Kotani, On the magnetic moment of complex ions. (I), *J. Phys. Soc. Jpn.* **4**, 293 (1949).

[38] B. N. Figgis, J. Lewis, R. S. Nyholm, and R. D. Peacock, The magnetic properties of some  $d^3$ ,  $d^4$  and  $d^5$  configurations, *Discuss. Faraday Soc.* **26**, 103 (1958).

[39] H. Lu, J. R. Chamorro, C. Wan, and T. M. McQueen, Universal single-ion physics in spin-orbit-coupled  $d^5$  and  $d^4$  ions, *Inorg. Chem.* **57**, 14443 (2018).

[40] J. B. Goodenough, Spin-orbit-coupling effects in transition-metal compounds, *Phys. Rev.* **171**, 466 (1968).

[41] D. K. C. MacDonald, *Thermoelectricity: An Introduction to the Principles* (John Wiley and Sons, New York, London, 1962).

[42] J. S. Zhou and J. B. Goodenough, Heterogeneous electronic structure in  $\text{CaVO}_3$ , *Phys. Rev. B* **54**, 13393 (1996).

[43] J. S. Zhou, L. G. Marshall, and J. B. Goodenough, Mass enhancement versus Stoner enhancement in strongly correlated metallic perovskites:  $\text{LaNiO}_3$  and  $\text{LaCuO}_3$ , *Phys. Rev. B* **89**, 245138 (2014).

[44] J. S. Zhou, J. B. Goodenough, B. Dabrowski, P. W. Klamut, and Z. Bukowski, Probing the metal-insulator transition in  $\text{Ni(III)}$ -oxide perovskites, *Phys. Rev. B* **61**, 4401 (2000).

[45] J. G. Cheng, J. S. Zhou, J. B. Goodenough, J. A. Alonso, and M. J. Martínez-Lope, Pressure dependence of metal-insulator transition in perovskites  $\text{RNiO}_3$  ( $\text{R} = \text{Eu, Y, Lu}$ ), *Phys. Rev. B* **82**, 085107 (2010).

[46] E. Langenberg, E. Ferreiro-Vila, V. Leborán, A. O. Fumega, V. Pardo, and F. Rivadulla, Analysis of the temperature dependence of the thermal conductivity of insulating single crystal oxides, *APL Mater.* **4**, 104815 (2016).

[47] D. G. Cahill, S. K. Watson, and R. O. Pohl, Lower limit to the thermal conductivity of disordered crystals, *Phys. Rev. B* **46**, 6131 (1992).

*Correction:* The middle initial of the fourth author was incorrect and has been rectified.